Article

Electrochemistry of Individual Molecules in Zeptoliter Volumes

Peng Sun, and Michael V. Mirkin

More About This Article

Additional resources and features associated with this article are available within the HTML version:

- Supporting Information
- Links to the 2 articles that cite this article, as of the time of this article download
- Access to high resolution figures
- Links to articles and content related to this article
- Copyright permission to reproduce figures and/or text from this article

View the Full Text HTML

Electrochemistry of Individual Molecules in Zeptoliter Volumes

Peng Sun and Michael V. Mirkin*

Department of Chemistry and Biochemistry, Queens College - CUNY, Flushing, New York 11367

Received December 13, 2007; E-mail: mmirkin@qc.cuny.edu

Abstract: Electrochemical experiments were carried out in a nanometer-sized cylindrical thin layer cell (TLC) formed by etching the surface of a disk-type platinum nanoelectrode (5- to 150-nm radius). Using high frequency ac voltage, the surface of such an electrode was etched to remove a very thin ($\geq$1-nm-thick) layer of Pt. The resulting zeptoliter-scale cavity inside the glass sheath was filled with aqueous solution containing redox species, and the etched electrode was immersed in a dry (no external solution) pool of mercury to produce a TLC. Several approaches based on steady-state voltammetry and scanning electrochemical microscopy (SECM) were developed to independently evaluate the electrode radius and the etched volume. The number of redox molecules in the TLC could be varied between one and a few hundred by changing its volume and solution concentration. In this way, the transition between a random and deterministic number of trapped molecules was observed. High quality steady-state voltammograms of $\geq$1 molecules were obtained for different neutral and charged redox species and different concentrations of supporting electrolyte. The analysis of such voltammograms yields information about mass transfer, adsorption, electron transfer kinetics, and double-layer effects on the nanoscale.

1. Introduction

Recent advances in nanoelectrochemistry provided new tools for single molecule experiments and measurements in microscopic volumes.[1] Such experiments offer important advantages over large-scale measurements ranging from analyzing ultrasmall samples[2] to obtaining physicochemical data not averaged over a large population of molecules.[3] In previous single molecule electrochemical studies,[4–7] the molecule of interest was singled out of a large number of species present in the system. Here we introduce a nanometer-sized electrochemical thin layer cell (TLC) in which the total number of redox molecules can be varied between one and a few hundred. One goal is to check if the processes occurring in a nanometer-sized cell and involving just a few molecules follow conventional electrochemical theory. A complementary question is whether any new phenomena can be observed in the nanoscale system that had not been accessible by macroscopic electrochemical approaches.

The nanocells used in this work are somewhat related to much larger (micrometer-sized) TLCs produced earlier by immersing an ultramicroelectrode (UME) in mercury.[8] When an UME penetrates a pool of mercury, a thin layer of the electrolyte gets trapped between the UME and the Hg surface forming a TLC.[8a] Although quantitative kinetic experiments were carried out inside the Hg pool, the trapped solvent layer in ref 8 was relatively thick, and its thickness was hard to control. Here, a different approach is used to prepare Hg-based nano-TLCs with the controlled volume and thickness.

Recently,[9a] we developed the methodology for preparation and characterization of the disk-type, polished nanoelectrodes with a radius $a \geq 3$ nm. As demonstrated by White and co-workers, flat nanoelectrodes can be etched to produce a nanopore.[10] By using a high-frequency (e.g., 2 MHz) ac etching current, we prepared slightly recessed nanoelectrodes with a recess depth of $\gtrsim 3$ nm.[9b] The etched electrodes were characterized by combination of voltammetry and scanning electrochemical microscopy (SECM) to determine the radius and the effective depth of the recess. In the present work, the etched Pt nanoelectrodes (Figure 1A) are filled with an aqueous solution containing redox species and immersed in the pool of dry (no

(1) Murray, R. W. *Chem. Rev.*, in press.
(2) (a) Clark, R. A.; Hietpas, P. B.; Ewing, A. G. *Anal. Chem.* **1997**, *69*, 259. (b) Troyer, K. P.; Wightman, R. M. *Anal. Chem.* **2002**, *74*, 5370.
(3) Bard, A. J.; Fan, F.-R. F. *Acc. Chem. Res.* **1996**, *29*, 572.
(4) (a) Fan, F.-R. F.; Bard, A. J. *Science* **1995**, *267*, 871. (b) Fan, F.-R. F.; Kwak, J.; Bard, A. J. *J. Am. Chem. Soc.* **1996**, *118*, 9669.
(5) Zhang, J.; Chi, Q.; Albrecht, T.; Kuznetsov, A. M.; Grubb, M.; Hansen, A. G.; Wackerbarth, H.; Welinder, A. C.; Ulstrup, J. *Electrochim. Acta* **2005**, *50*, 3143.
(6) Donner, S.; Li, H.-W.; Yeung, E. S.; Porter, M. D. *Anal. Chem.* **2006**, *78*, 2816.
(7) Palacios, R. E.; Fan, F.-R. F.; Bard, A. J.; Barbara, P. F. *J. Am. Chem. Soc.* **2006**, *128*, 9028.
(8) (a) Mirkin, M. V.; Bard, A. J. *J. Electrochem. Soc.* **1992**, *139*, 3535. (b) Mirkin, M. V.; Bulhões, L. O. S.; Bard, A. J. *J. Am. Chem. Soc.* **1993**, *115*, 201.
(9) (a) Sun, P.; Mirkin, M. V. *Anal. Chem.* **2006**, *78*, 6526. (b) Sun, P.; Mirkin, M. V. *Anal. Chem.* **2007**, *79*, 5809.
(10) (a) Zhang, B.; Zhang, Y.; White, H. S. *Anal. Chem.* **2004**, *76*, 6229. (b) Zhang, B.; Zhang, Y.; White, H. S. *Anal. Chem.* **2006**, *78*, 477. (c) Zhang, Y.; Zhang, B.; White, H. S. *J. Phys. Chem. B* **2006**, *110*, 1768. (d) Wang, G.; Bohaty, A. K.; Zharov, I.; White, H. S. *J. Am. Chem. Soc.* **2006**, *128*, 13553. (e) Wang, G.; Zhang, B.; Wayment, J. R.; Harris, J. M.; White, H. S. *J. Am. Chem. Soc.* **2006**, *128*, 7679. (f) White, R. J.; Zhang, B.; Daniel, S.; Tang, J. M.; Ervin, E. N.; Cremer, P. S.; White, H. S. *Langmuir* **2006**, *22*, 10777. (g) Zhang, B.; Galusha, J.; Shiozawa, P. G.; Wang, G.; Bergren, A. J.; Jones, R. M.; White, R. J.; Ervin, E. N.; Cauley, C. C.; White, H. S. *Anal. Chem.* **2007**, *79*, 4778.
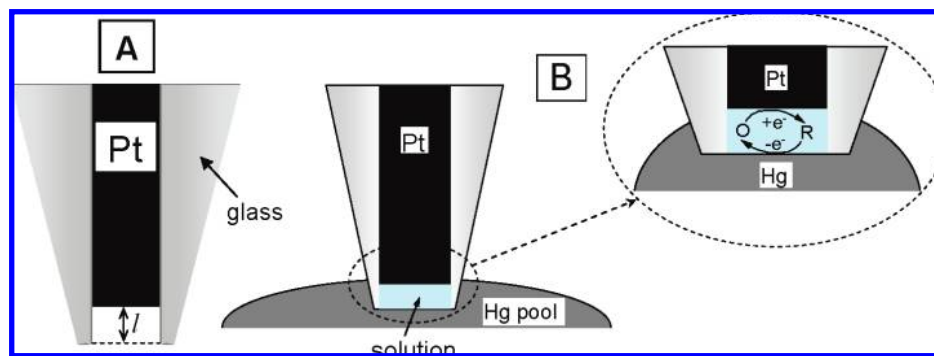
Figure 1. Schematic representation of a recessed nanoelectrode (A) and TLC prepared by immersing an etched Pt nanoelectrode into the pool of Hg (B). The inset shows a thin water layer trapped inside the glass sheath. Oxidized form of the mediator is reduced at Pt UME and reoxidized at the Hg surface.

external solution) mercury to produce nano-TLCs with variable and controllable spatial dimensions (Figure 1B). The volume of such a cell can be as small as <1 zeptoliter (i.e., 10^{-21} L), and the number of redox molecules in it can be varied from zero to a few hundred.

The inset in Figure 1B shows the scheme of a TLC voltammetric experiment. Similarly to feedback mode SECM experiments,[8] the mediator species is reduced (or oxidized) at the Pt surface and regenerated at the Hg surface. When the TLC thickness (l) is small, the feedback process can provide sufficient amplification to measure the current produced by oxidation/reduction of a few redox molecules.[4]

2. Experimental Section

2.1. Chemicals. Triple-distilled mercury (Bethlehem Apparatus Company Hellertown, Pennsylvania) was treated with oxygen-saturated nitric acid for 24 h and filtered before use. Hexaamineruthenium(III) chloride ($Ru(NH_3)_6Cl_3$, 99%) was obtained form Strem Chemicals (Newburyport, MA), $K_3Fe(CN)_6$ (99%) was from Sigma, and $Na_4Fe(CN)_6$ was from Fisher Scientific. Ferrocenemethanol ($FcCH_2OH$, 97%) from Aldrich (Milwaukee, WI) was recrystallized twice from acetonitrile. Potassium hexachloroiridate(III) was from Alfa Aesar. Potassium nitrate (99+%, Aldrich) was recrystallized twice from water and used as a supporting electrolyte. $Na_4Ru(CN)_6$ was synthesized as reported previously,[11] recrystallized several times from methanol/water, and dried under vacuum overnight at 50 °C. Aqueous solutions were prepared from deionized water (Milli-Q, Millipore Co.).

2.2. Electrodes and Electrochemical Cells. Slightly recessed Pt nanoelectrodes were prepared as described in ref 9b. Briefly, disk-type, flat polished nanoelectrodes with *RG* (i.e., the ratio of the insulating sheath radius to *a*) between 5 to 20 were fabricated according to the previously reported procedures.[9a] The electrode radius was evaluated from the diffusion plateau current of a steady-state voltammogram

$$i_d = 4FDc^*a \qquad (1)$$

where F is the Faraday constant, and D and c^* are the diffusion coefficient and the bulk concentration of the redox species, respectively. The determined a value could be independently validated by SECM measurements.[9a]

The electrode was rinsed several times by distilled water and dried in the oven at 120 °C for 1 h, and the surface of insulating glass was silanized by immersing it in 2 mL of dry toluene containing 100 μL of octadecyltrimethoxysilane (90%, Aldrich) for 10 h. The silanized UME was rinsed several times by acetone, dried at 80 °C for 2−3 h, and etched in solution containing 60% (by

volume) distilled water, 30% 5 M $CaCl_2$, and 10% HCl, with an alternating current of 1.5 V amplitude, 2 MHz frequency (Keithley, 3940, multifunctional synthesizer).[9b] After etching, the outer glass surface remained hydrophobic, while the inner surface of the etched cavity was hydrophilic. Thus, one could fill the inner hydrophilic cavity with aqueous solution without forming a film of water on the hydrophobic outer surface of the probe.[12]

To find the recess depth, steady-state voltammograms at the etched electrode were obtained in the same solution that was used previously to evaluate a. The l value was found from the ratio of the plateau currents measured after and before etching ($I_{T,\infty} = i_{T,\infty}/i_d$) using eq 2[9b]

$$H = 2.83649 \exp(I_{T,\infty}) + 0.78227/I_{T,\infty} - 3.14644I_{T,\infty} - 1.74378I_{T,\infty}^{2.5} - 3.59162 \quad (2)$$

where $H = l/a$ (see ref 13a and 13b for detailed discussion of theory of recessed electrodes).

To form a TLC, the etched electrode was first immersed in solution containing redox species of interest and supporting electrolyte, then removed from that solution, and inserted into the pool of dry mercury. The insertion depth was typically between 30 and 100 μm. A Hg pool was formed in a 1.2-cm-diameter glass cell that was placed in a plastic box with a small hole for the UME insertion. The bottom of the box was covered by a layer of water to maintain a humid atmosphere. This was essential to prevent the evaporation of water from the nanocavity. To verify that the formed TLC was isolated from the environment, in some experiments a portion of the Hg surface, several millimeters away from the UME, was covered by aqueous solution. This solution either had the same composition as the solution inside TLC or contained only supporting electrolyte, or a different kind of redox species. In all cases, the TLC voltammetric response (see below) was essentially unaffected by the presence of an external solution on the Hg surface.
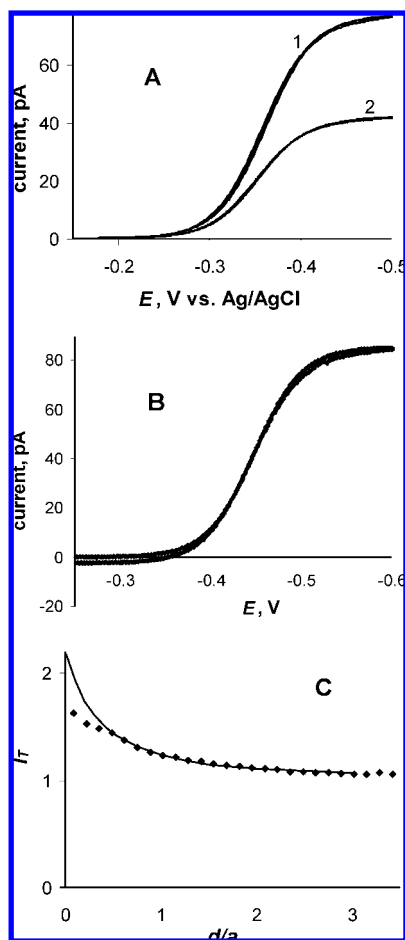
2.3. Instrumentation and Procedures. Voltammetry and SECM measurements were performed in a two-electrode mode with either a commercial Ag/AgCl electrode or a Hg pool serving as a reference electrode. Cyclic voltammograms were obtained using either an EI-400 bipotentiostat (Ensman Instruments, Bloomington, IN) or a BAS-100B electrochemical analyzer (Bioanalytical Systems, West Lafayette, IN). In TLC voltammograms, E is the potential of the recessed Pt electrode measured with respect to Hg. The potential sweep rate was 30 mV/s.

(11) Krause, R. A.; Violette, C. *Inorg. Chim. Acta* **1986**, *113*, 161.

(12) Shao, Y.; Mirkin, M. V. *Anal. Chem.* **1998**, *70*, 3155.
(13) (a) Bartlett, P. N.; Taylor, S. L. *J. Electroanal. Chem.* **1998**, *453*, 49. (b) Amatore, C.; Oleinick, A. I.; Svir, I. *J. Electroanal. Chem.* **2006**, *597*, 77.
(14) (a) Hubbard, A. T.; Anson, F. C. In *Electroanalytical Chemistry*; Bard, A. J., Ed.; Marcel Dekker: New York, 1970; Vol. 4, p 129. (b) Mirkin, M. V.; Bard, A. J. *Anal. Chem.* **1992**, *64*, 2293. (c) For discussion of the validity of eq 8, see subsection "Rectifying response of TLCs and pinned potential of Hg".

Figure 2. Voltammograms (A and B) and an SECM approach curve (C) obtained with a 150-nm Pt electrode. (A) Voltammograms were obtained before (1) and after etching (2). A TLC voltammogram (B) and a current−distance curve (C) were obtained with the same etched electrode. Theoretical curve (solid line in C) was calculated from eq 10[9b] with a = 150 nm and H = 0.664. Solution contained 2 mM Ru(NH$_3$)$_6$Cl$_3$ and 0.2 M KNO$_3$.

SECM experiments were carried out using a home-built instrument described previously.[9b] The 3D stage and the substrate were mounted on an optical table (Newport) suspended with pressured nitrogen to dampen mechanical vibrations. All experiments were carried out at room temperature (23 ± 2 °C) inside a Faraday cage. To obtain an approach curve, the tip was biased at a potential where the oxidation (or reduction) of the mediator species occurred at a diffusion-controlled rate. The Au substrate was always unbiased. The procedures used to bring a recessed tip close to the conductive surface and achieve a proper tip/substrate alignment were discussed previously.[9b]

3. Results and Discussion

3.1. TLC Voltammetry and Evaluation of Its Thickness and Volume. Figure 2 shows steady-state voltammograms of 2 mM Ru(NH$_3$)$_6^{3+}$ obtained at the same Pt nanoelectrode before etching (curve 1 in A), after etching (curve 2 in A), and in the TLC formed inside the Hg pool (B). Using eq 1, one can find a = 150 nm from curve 1 (Figure 1A). From curve 2, $I_{T,\infty}$ = 0.535; the corresponding H value found from eq 2 is 0.664, and the recess depth is l_{CV} = aH = 99.6 nm. An SECM current vs distance curve (Figure 2C) was obtained with the same recessed UME used as a tip and approaching a gold substrate. The experimental curve (symbols) was fitted to the theory (solid

Table 1. Recess Depth (l_{CV}) and TLC Thickness (l_{TLC}) Values and the Expected Numbers of Trapped Redox Molecules (N) for Electrodes of Different Radii (a)[a]

electrode no.	a, nm	l_{CV}, nm[b]	l_{TLC}, nm[c]	N[d]
1	115.0	10.3	9.9	256
2	83.2	10.4	9.7	136
3	69.8	14.9	14.0	137
4	15.2	12.3	9.2	5.4
5	14.4	7.1	5.4	2.8
6	14.1	7.0	8.6	2.6
7	13.9	12.0	10.1	4.4
8	12.5	7.8	7.3	2.3
9	7.2	2.3	6.3	0.2

[a] Solution contained 1 mM FcCH$_2$OH and 0.2 M KNO$_3$. [b] Equation 2. [c] Equation 3. [d] Equation 4.

line)[9b] using a and H found from voltammetry to confirm the validity of these values. As discussed earlier,[9b] the experimental approach curve fits the theory up to the point where the tip's insulating sheath touches the substrate surface ($d \cong 0.4a$). The diffusion limiting current in the TLC voltammogram (Figure 2B) is significantly higher than that measured at the same electrode in the bulk solution after etching (Figure 2A, curve 2).

This increase (positive feedback) is due to the regeneration of the mediator at the Hg surface (Figure 1B, inset). Assuming the cylindrical geometry of the TLC and equal diffusion coefficients of the oxidized and reduced forms of the redox species, the diffusion limiting current is[14a]

$$i_{TCL} = \frac{\pi a^2 FDc^*}{l_{TLC}} \quad (3)$$

where the radii of Pt and Hg electrodes are both equal to a and l_{TLC} is the distance between them.[14a] Substituting a = 150 nm in eq 3, one obtains l_{TLC} = 107 nm. This value is in good agreement (within ~7%) with l_{CV} found for the same etched UME from solution voltammetry (Figure 2A) and SECM measurements (Figure 2C).

A larger set of data were obtained to check the agreement between the l_{TLC} and l_{CV} values using a ferrocenemethanol redox mediator (Table 1). For each electrode, the expected number of trapped redox molecules is

$$N = V_{TLC}c^*N_A \quad (4)$$

where $V_{TLC} = \pi a^2 l_{CV}$ is the volume of the etched cavity, c^* = 10^{-6} mol/cm^3 is the concentration of FcCH$_2$OH in solution, and N_A is the Avogadro number. There is a close agreement between the l_{CV} and l_{TLC} values for each electrode in Table 1 except electrode 9, where the number of expected molecules (0.2) is nonphysical. The average difference between the l_{CV} and l_{TLC} values for the first eight electrodes in Table 1 is only 14%. The independently determined recess depth and TLC thickness agree well even for very small electrode 8 (V_{TLC} = 3.8 zL, i.e., 3.8 ×10^{-21} L).

A good agreement between the apparent TLC thickness and the recess depth indicates that the solution completely fills the etched cavity without either bulging outside or leaving space for Hg penetration inside the cavity. The observed agreement also suggests that the effective concentration of FcCH$_2$OH inside the TLC is similar to its concentration in the filling solution. The same conclusion can be drawn from the fact that essentially the same l_{TLC} value was found from voltammograms obtained with different bulk concentrations of redox species and from linear i_{TCL} vs c^* dependences (see below).
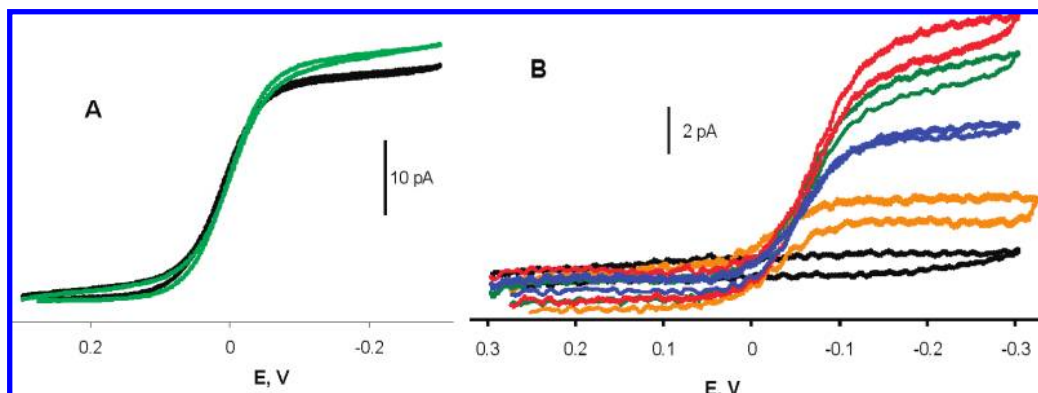
Figure 3. Reproducibility of voltammograms obtained in a relatively large TLC (A) and random sampling of single molecules in a small TLC (B). $a = 115$ nm (A) and 15.2 nm (B). $l_{CV} = 10.3$ nm (A) and 6.8 nm (B). The voltammograms were obtained by repeatedly transferring an etched Pt nanoelectrode from 1 mM FcCH$_2$OH solution to a mercury pool.

3.2. Sampling Single Molecules. In Table 1, the apparent number of FcCH$_2$OH molecules (N) varies between several hundreds and less than one. When V_{TLC} is relatively large, one can expect to trap a similar number of molecules every time when the same etched nanoelectrode is filled with the same solution and immersed in Hg. Such a "deterministic" behavior was indeed observed: essentially reproducible cyclic voltammograms were obtained by withdrawing a relatively large UME from mercury, immersing it in the same filling solution, and then reinserting in Hg (Figure 3A; $a = 115$ nm, $l_{CV} = 10.3$ nm, $N = 258$ FcCH$_2$OH molecules). The similarity of the plateau currents (within ~5%) also points to a good reproducibility of the l_{TLC} value.

In contrast, when N is small (e.g., <5), large uncertainty can be expected in the sampling process. An example of "random" sampling is shown in Figure 3B. Using $a = 15.2$ nm, $l_{CV} = 6.8$ nm, and $c^* = 1$ mM, eq 4 yields $N = 2.96$. Five voltammograms in Figure 3B were obtained by repeatedly immersing this electrode in Hg. Assuming $l_{TLC} \cong l_{CV} = 6.8$ nm, the limiting current values in Figure 3B correspond to $N = 0$ (black), 1.1 (orange), 2.1 (blue), 3.0 (green), and 3.6 (red), i.e., to zero, one, two, three, and four molecules (within the limits of our experimental error) trapped inside the nano-TLC.

Since the charge carried by an electron is 1.6×10^{-19} C, a single molecule has to collide with each electrode ~10^7 times per second to carry a 2 pA current (orange curve in Figure 3B). By comparison the characteristic diffusion time for this system is

$$t_d = (2l)^2/D = 1.8 \times 10^{-7} \text{ s} \qquad (5)$$

in a good agreement with the calculated collision frequency.

It is interesting to compare the voltammograms in Figure 3B to the results of single molecule electrochemical experiments reported by Fan et al.[4] In those experiments, a Pt nanotip was recessed inside a small compartment formed within the wax insulator. A TLC with the dimensions similar to those of ours was produced by pushing such an electrode against a conducting surface. However, the voltammograms and current–time dependencies recorded in ref 4 exhibited high-amplitude current fluctuations. The fluctuations were attributed to migration of single electroactive molecules in and out of the TLC, which was not completely isolated from the surrounding solution. In our setup, electroactive species are confined to the Pt/Hg gap, and there is no outer solution.

Therefore, there are no significant current fluctuations, and fully reproducible steady-state voltammograms can be obtained by cycling the applied voltage.

Although one would not expect a hydrophobic mercury surface to be covered with water, the absence of a thin water film on Hg is hard to ascertain. However, if such a film was present, it was completely isolated from the thin layer cell. In our control experiments, a portion of Hg surface was covered with an aqueous solution containing different redox species, but those species have never been detected in the TLC. Also, an excellent agreement between the l_{TLC} and l_{CV} values in Table 1 indicates that the sampled solution was not diluted by water coming from the Hg surface inside the nanocavity.

3.3. Adsorption of Individual Molecules. All FcCH$_2$OH and Ru(NH$_3$)$_6^{3+/2+}$ solutions used in TLCs (Figures 2 and 3) contained either 1 mM or 2 mM of redox species. In contrast, the voltammograms of Ru(CN)$_6^{4-/3-}$ (Figure 4A) show no waves at $c^* = 1$ mM, 2 mM, or 3 mM (curves 1–3). Since higher concentrations of Na$_4$Ru(CN)$_6$ yielded regular voltammetric waves, the lack of a measurable current indicates that no redox species were present in the Pt/Hg gap at $c^* \leq 3$ mM. For the TLC employed in Figure 4A, the expected number of Na$_4$Ru(CN)$_6$ molecules is $N = 70 \cdot c^*$, where c^* is expressed in mM. So, for $c^* = 3$ mM $N = 210$ molecules, and the possibility of $N = 0$ is unrealistic. The apparent decrease in N can be explained by adsorption of redox species on the Hg surface (the fast-scan voltammograms of Na$_4$Ru(CN)$_6$ at Pt electrodes showed no signs of adsorption). An adsorbed redox species does not cycle between Pt and Hg electrodes and thus cannot contribute to the measured steady-state current. Therefore, adsorption results in a decrease in the apparent number of redox species in the TLC. The number of adsorbed ions is approximately 70, 140, and 210 for curves 1, 2, and 3 in Figure 4A. The last number apparently corresponds to the surface saturation, and the linear i_{TLC} vs c^* dependence (Figure 4B) indicates that no further adsorption of redox species occurs at $c^* > 3$ mM. Thus, the maximum surface coverage, Γ_{max}, is ~10^{-11} mol/cm^2.

The number of adsorbed redox species corresponding to the maximum coverage is

$$N_{max} = \pi a^2 \Gamma_{max} N_A \qquad (6)$$
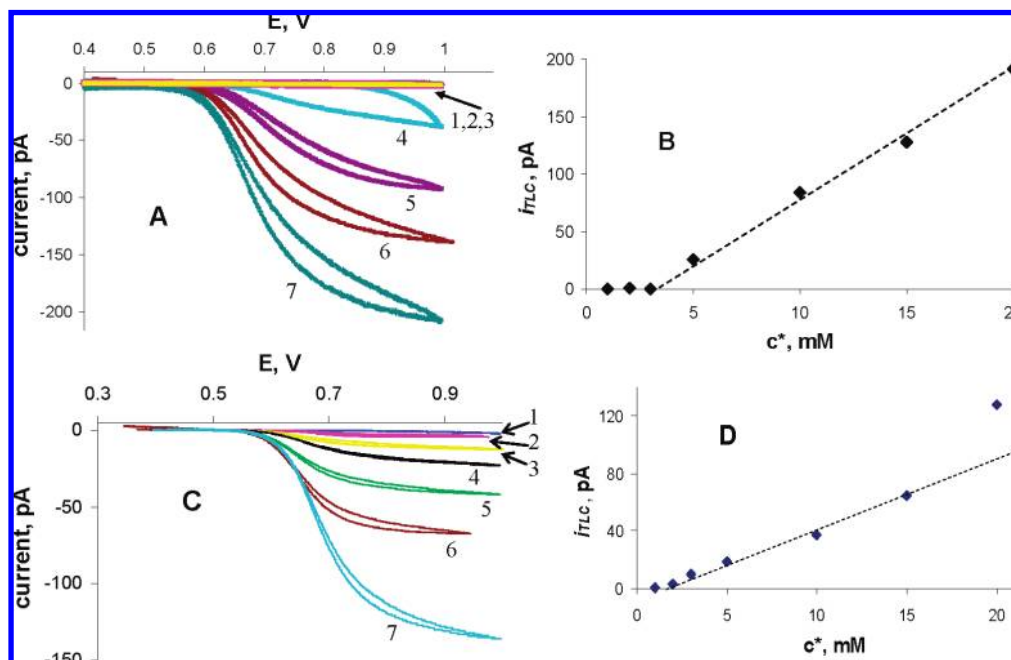
Figure 4. Voltammograms of $Na_4Ru(CN)_6$ obtained in two different TLCs (A and C) and corresponding concentration dependences of the plateau current (B and D). $a = 51.4$ nm (A) and 46 nm (C). $l_{CV} = 14$ nm (A) and 30 nm (C). (A and C) c*, mM was as follows: 1 (1), 2 (2), 3 (3), 5 (4), 10 (5), 15 (6), and 20 (7). Solutions also contained 0.2 M KNO_3.
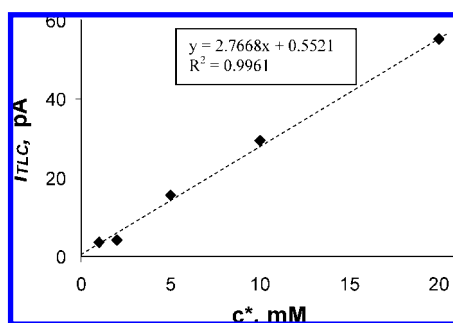
Figure 5. Concentration dependence of the plateau current obtained from TLC voltammograms of K_3IrCl_6. $a = 97.4$ nm, $l_{CV} = 26.7$ nm. Supporting electrolyte was 0.2 M KNO_3.

A TLC voltammetric wave should be measurable if the number of trapped redox species exceeds N_{max}. The combination of eqs 4 and 6 yields

$$c_{max}^* = \Gamma_{max}/l \qquad (7)$$

where c_{max}^* is the maximum concentration of redox species in solution at which a TLC voltammogram is still flat. This concentration should be inversely proportional to l and independent of a.

A family of $Ru(CN)_6^{4-/3-}$ voltammograms in Figure 4C was obtained in a TLC with $a = 46$ nm and a thickness approximately two times larger than that in Figure 4A, $l_{CV} = 30$ nm. Qualitatively, this data are similar to those in Figure 4A: no measurable current at low c* and a linear i_{TLC} vs c* dependence at higher $Na_4Ru(CN)_6$ concentrations. However, the c_{max}^* in Figure 4C is between 1 mM and 2 mM, i.e., about one-half of $c_{max}^* = 3$ mM in Figure 4A, in accordance with the ratio of corresponding l_{CV} values.

Figure 5 shows the i_{TLC} vs c* dependence obtained from TLC voltammograms of K_3IrCl_6. $IrCl_6^{3-/2-}$ redox mediator is in many ways similar to $Ru(CN)_6^{4-/3-}$: both oxidized and reduced forms
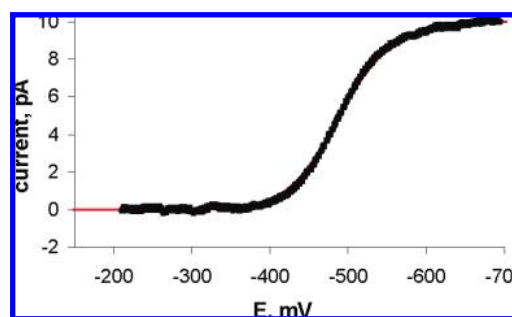

Figure 6. Experimental (symbols) and theoretical (solid line) voltammograms of a single $Ru(NH_3)_6^{3+/2+}$ species at the etched Pt electrode immersed in Hg. $a = 8.2$ nm, $l_{CV} = 1.2$ nm. Theoretical curve was calculated from eq 8 with $k^o = 8.55$ cm/s and $\alpha = 0.58$. Solution contained 2 mM $Ru(NH_3)_6Cl_3$ and 0.2 M KNO_3.

are multicharged anionic species; both couples have high positive formal potentials (644 mV and 720 mV vs Ag/AgCl, respectively) and exhibit quasi-reversible electron transfer kinetics. However, $IrCl_6^{3-/2-}$ species apparently do not adsorb on Hg, and the i_{TLC} vs c* plot in Figure 5 is linear with the zero intercept.

Unlike Hg, the glass surface gets pre-exposed to solution when an etched electrode is immersed in it. Because the same solution is sampled within the TLC, no additional adsorption/desorption is expected to occur at the inner glass wall. Although the Pt surface is also exposed to solution during the sampling process, the surface coverage of Pt electrode within TLC may change as a function of it potential and affect the solution concentration of redox species and thus the diffusion current. The adsorption effects in nano-TLCs are important because of a very large surface area to volume ratio.

3.4. Heterogeneous Electron Transfer Kinetics. The voltammogram in Figure 6 was obtained at the 8.2-nm-radius electrode immersed in Hg. The filling solution contained 2 mM $Ru(NH_3)_6Cl_3$ and 0.2 M KNO_3. With $l_{CV} = 1.2$ nm and $V_{TLC} =$
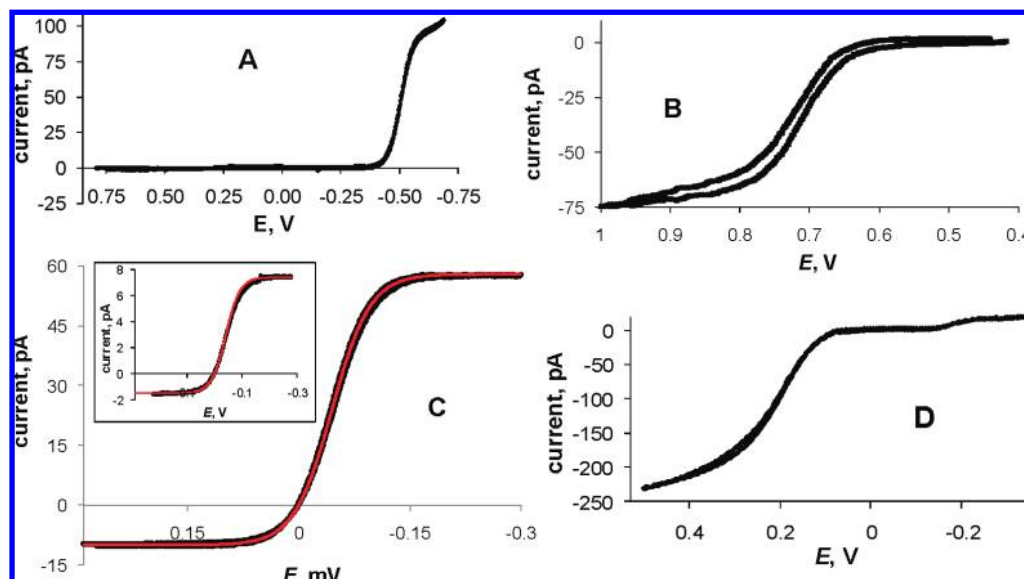
Figure 7. TLC voltammograms of different redox mediators. The solution compositions and cell dimensions are as follows: (A) 2 mM Ru(NH₃)₆Cl₃; $a = 117$ nm, $l_{CV} = 57$ nm; (B) 5 mM K₃IrCl₆; $a = 25$ nm, $l_{TLC} = 14$ nm; (C) 1 mM FcCH₂OH; $a = 58$ nm, $l_{TLC} = 11.7$ nm; (inset) $a = 14.6$ nm, $l_{TLC} = 3.5$ nm; red lines are theoretical curves calculated from eq 9; (D) 5 mM K₄Fe(CN)₆, 5 mM K₃Fe(CN)₆; $a = 98$ nm, $l_{CV} = 115$ nm. In all solutions, supporting electrolyte was 0.2 M KNO₃.

2.5×10^{-22} L, the expected number of Ru(NH₃)₆Cl₃ molecules is 0.3. Thus, the current in Figure 6 was most likely produced by oxidation/reduction of a single molecule. A good fit can be seen between the experimental voltammogram (symbols) and the theoretical curve (solid line) calculated from eq 8 assuming equal diffusion coefficients of the oxidized and reduced forms:[14b]

$$I(E) = \frac{i_{TLC}}{1 + \exp[(E - E^{o'})F/RT] + m/k^o \, \exp[-\alpha(E - E^{o'})F/RT]} \quad (8)$$

where $i(E)$ is the steady-state current at a given potential, $E^{o'}$ is the formal potential, k^o is the standard rate constant, α is the transfer coefficient, and $m = i_{TLC}/\pi a^2 Fc$ is the effective mass transfer coefficient.[14c]

The kinetic parameters extracted from Figure 6, i.e., $k^o = 8.6$ cm/s and $\alpha = 0.58$, are reasonably close to those obtained recently in voltammetric and SECM experiments at polished nanoelectrodes ($k^o = 17.0$ cm/s and $\alpha = 0.45$).[9a] The use of 0.5 M KCl as a supporting electrolyte in ref 9a is a likely reason for a somewhat higher measured rate constant.[15] In this work, we have not used KCl to avoid calomel formation on the Hg surface. Clearly, a much larger set of data is needed to compare the results of single molecule kinetic experiments to those obtained in the bulk solution and explore possible effects of diffuse layer overlap and unusual mass-transfer conditions in nano-TLCs.[16–18] This work is currently in progress in our laboratory.

3.5. Unusual Electrochemical Phenomena in Nano-TLCs. In experiments reported above, the responses of nanometer-sized TLCs containing just a few redox molecules were in accordance with conventional electrochemical theory. Here we report several

experimental observations that reflect the differences between nanoscopic and macroscopic systems.

3.5.1. Rectifying Response of TLCs and Pinned Potential of Hg. In the absence of kinetic limitations, steady-state voltammetric waves obtained by application of a linear voltage sweep between two working electrodes of a TLC are supposed to be symmetrical with similar oxidation and reduction plateau currents and $i = 0$ corresponding to zero applied voltage.[14a] No such waves can be seen in Figures 2B, 3B, and 4. The current rectification is evident in the TLC voltammogram of Ru(NH₃)₆Cl₃ in Figure 7A obtained over a wide range of voltages (from +0.8 to −0.7 V) with a well-defined wave obtained at negative voltages (i.e., Pt potential negative vs Hg) and essentially no current flowing at positive E up to +0.8 V. To understand this response, one needs to notice that the steady-state current can flow in a TLC only if a redox species is oxidized at one working electrode and reduced at the second electrode. In Figure 7A, Ru(NH₃)₆³⁺ is reduced at the Pt nanoelectrode and Ru(NH₃)₆²⁺ is oxidized at the Hg surface, but the opposite process (i.e., oxidation at Pt and reduction at Hg) does not occur. Since this electron transfer reaction is essentially Nernstian at both Pt and Hg, the observed response indicates that the application of external voltage as high as 0.8 V does not make the Hg potential sufficiently negative to reduce Ru(NH₃)₆³⁺.

The current rectification in the opposite direction was observed for hexachloroiridate (Figure 7B) and hexacyanoruthenate (Figure 4C) species; i.e., in both cases the oxidation reaction occurred at Pt, and the reduction, at Hg, but not vice versa. The rectifying behavior of TLCs can be explained assuming that the Hg/water interface is not polarizable and the potential of Hg is pinned at a fixed value, $E^{o'}_{Ru(NH_3)_6} < E_{Hg} < E^{o'}_{IrCl_6}$, where $E^{o'}_{Ru(NH_3)_6} = -302$ mV vs AgCl and $E^{o'}_{IrCl_6} = 644$ mV vs AgCl are the formal potentials of the two redox couples measured in 0.2 M KNO₃ solutions.

A better estimate for E_{Hg} can be obtained from the voltammogram of FcCH₂OH (Figure 7C). This curve comprises both oxidation and reduction waves, and the height of the wave

(15) Penner, R. M.; Heben, M. J.; Longin, T. L.; Lewis, N. S. *Science* **1990**, *250*, 1118.
(16) Smith, C. P.; White, H. S. *Anal. Chem.* **1993**, *65*, 3343.
(17) He, R.; Chen, S.; Yang, F.; Wu, B. *J. Phys. Chem. B* **2006**, *110*, 3262.
(18) Chen, J.; Aoki, K. *Electrochem. Commun.* **2002**, *4*, 24.

corresponding to the reduction at Pt and oxidation at the Hg electrode is ~5 times the limiting current value for the reverse reaction. Assuming that oxidation/reduction of ferrocenemethanol at both electrodes is Nernstian, and $E_{Hg} = const$, one can express steady-state voltammetric current by eq 9 (see Supporting Information):

$$I(E) = \frac{AFD_O c^* [1 - \exp(EF/RT)]}{l[\exp(E^{o'}F/RT) + \gamma \exp(EF/RT)][\exp(E^{o'}F/RT) + \gamma]} \quad (9)$$

where $A = \pi a^2$ is the electrode surface area, E is the applied voltage, $\gamma = D_O/D_R$; $c^* = (\gamma c_O^* + c_R^*)$; D_O and D_R, and c_O^* and c_R^* are the diffusion coefficients and concentrations of redox species in the filling solution; and the formal potential of the redox couple, $E^{o'}$ is expressed on the voltage scale (i.e., vs $E = 0$ point).

An excellent fit between the experimental data (symbols) and the theory (solid line calculated from eq 9) in Figure 7C was obtained with $E_{Hg} = E^{o'}_{FcCH_2OH} + 45$ mV $= 133$ mV vs Ag/AgCl. E_{Hg} was the only adjustable parameter: all other values (i.e., $a = 58$ nm, $l_{TLC} \cong l_{CV} = 11.7$ nm, and $D_R = D_O = 7.8 \times 10^{-6}$ cm^2/s) were determined independently, as discussed above. The inset in Figure 7 shows a steady-state voltammogram obtained in a much smaller TLC ($a = 11.5$ nm, $l_{TLC} = 3.5$ nm) fitted to eq 9 (solid line) with a very similar value of Hg potential, $E_{Hg} = E^{o'}_{FcCH_2OH} + 42$ mV. The E_{Hg} value obtained from Figure 2 ($E_{Hg} = E^{o'}_{Ru(NH_3)_6} + 440$ mV $= 138$ mV vs Ag/AgCl) agrees well with that found from Figure 7C. Equation 8, which used to fit an experimental voltammogram of hexaamineruthenium in Figure 6, is also based on the assumption of the pinned E_{Hg}.

It would not be possible to fit the voltammograms in Figure 7C without the assumption of the pinned Hg potential. In a conventional two-electrode TLC with a negligible ohmic drop, the applied voltage is equal to the difference of the potentials of two working electrodes.

$$E = E_{Pt} - E_{Hg} \quad (10)$$

Assuming that both electrodes are polarizable and both electrode reactions are Nernstian, with equal currents flowing at two working electrodes, the change in applied voltage (ΔE) contributes to both electrode potentials:

$$|\Delta E_{Pt}| = |\Delta E_{Hg}| = |\Delta E|/2 \quad (11)$$

In contrast, if the Hg potential is pinned,

$$\Delta E_{Pt} = \Delta E \quad (12)$$

and the current−voltage dependencies for these two cases should be completely different.

One should notice that the steady state in a nano-TLC is established within microseconds (or even nanoseconds) after the application of external voltage, and steady-state voltammograms do not tell us how it was attained. Accordingly, the observed rectification effect has nothing to do with the initial composition of the solution trapped in the TLC. This point is illustrated by Figure 7D, in which a TLC ($a = 98$ nm, $l_{CV} = 115$ nm) was loaded with solution containing 5 mM K$_4$Fe(CN)$_6$ and 5 mM K$_3$Fe(CN)$_6$. The resulting voltammetric wave corresponds to the oxidation ferrocyanide at Pt and its regeneration at Hg, and the reverse wave is very small. While the exact determination of E_{Hg} from this irreversible voltammogram is difficult, its value can be

estimated as ~100 mV vs Ag/AgCl, which is pretty close to the one found from Figure 7C.

Several possible reasons for a pinned potential of Hg were investigated including the formation of calomel, the presence of an aqueous film on the Hg/air interface, and the effect of atmospheric oxygen. However, the TLC behavior was essentially unaffected by the recrystallization of KNO$_3$ (to eliminate traces of Cl$^-$), covering a portion of the Hg surface with various solutions (see Experimental Section), or placing it in a N$_2$-filled container.

The nonpolarizability of the Hg electrode is related to the large total surface area of the mercury pool. Although only a nanometer-sized portion of the Hg surface is involved in TLC voltammetry, the charges injected into Hg can migrate to the macroscopic part of its surface exposed to air. Assuming the mercury pool to be a hemisphere with a radius $r = 0.5$ cm, its capacitance can be estimated as

$$C = 2\pi\varepsilon_o r = 0.28 \text{ pF} \quad (13)$$

where $\varepsilon_o = 8.854 \times 10^{-14}$ F/cm. This value is ~100 and ~2500 times the double layer capacitance of Pt electrodes with $a = 50$ and 10 nm, respectively (assuming $C_d = 20$ μF/cm^2). When double layer charging current is passed through the TLC, the same amount of charge (Q) has to be injected into both electrodes to preserve solution electroneutrality:

$$Q = C_{Hg}\Delta E_{Hg} = -C_{Pt}\Delta E_{Pt} \quad (14a)$$

and therefore

$$\Delta E_{Hg} = -\Delta E_{Pt} C_{Pt}/C_{Hg} \quad (14b)$$

When an external voltage, $E = 100$ mV, is applied to a nano-TLC, the expected change in E_{Hg} is ≤ 1 mV. Therefore, Hg acts an essentially nonpolarizable (quasi-reference) electrode.

3.5.2. Effect of Ionic Strength. Figure 8A and 8B show two families of TLC voltammograms of 1 mM FcCH$_2$OH obtained at the same Pt electrode ($a = 58$ nm, $l_{CV} = 12$ nm) immersed in Hg. These curves were obtained with different concentrations of KNO$_3$ supporting electrolyte. In Figure 8A, the electrolyte concentration was decreased from 1000 mM (green curve) to 100 mM (blue). The decrease in c_{KNO_3} caused almost no change in half-wave potential and a significant increase in diffusion current. The effect of the ionic strength was small for $c_{KNO_3} \geq 200$ mM, but a significant increase in i_{TLC} (~50%) occurred when c_{KNO_3} was reduced to 100 mM. In conventional electrochemical experiments in the bulk solution containing an excess of supporting electrolyte, the contribution of migration to the mass transfer rate is small,[19] and therefore the effect of c_{KNO_3} on the limiting current would be negligible. However, under TLC conditions, where a few hundred millivolt voltage is applied over a nanometer-thick solution layer, the migration contribution to the mass transport of FcCH$_2$OH$^+$ is significant even at a supporting electrolyte concentration as large as 100 times that of the redox species.

The lowering of c_{KNO_3} to 50 mM produced a striking effect: the wave height decreased by the factor of ~20 (black curve in Figure 8B). This change is especially surprising because $c_{KNO_3} = 50$ mM is still 50 times higher than the concentration

(19) (a) Bard, A. J.; Faulkner, L. R. *Electrochemical Methods: Fundamentals and Applications*; John Wiley & Sons, Inc.: New York, 2001. (b) Amatore, C. In *Physical Electrochemistry: Principles, Methods, and Applications*; Rubinstein, I., Ed.; Marcel Dekker: New York, 1995; p 131.
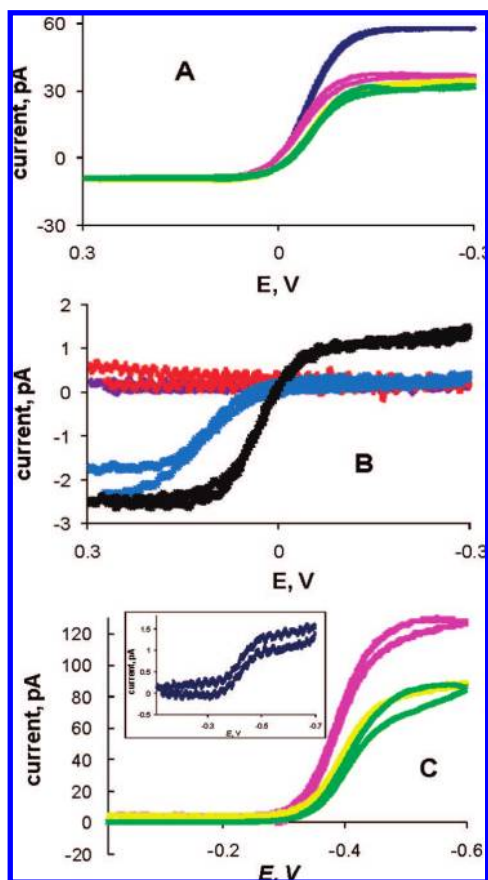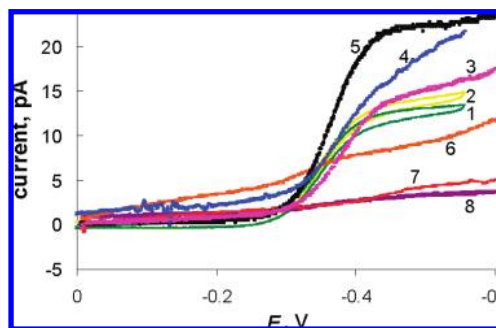
Figure 8. Effect of supporting electrolyte concentration on TLC voltammograms. (A) and (B) $a = 58$ nm, $l_{CV} = 12$ nm. Solution contained 1 mM FcCH$_2$OH. The concentration of KNO$_3$, mM: 1000 (green), 500 (yellow), 200 (pink), and 100 (blue) in panel A; 50 (black), 10 (blue), 3 (red), and 1 (purple) in panel B. (C) $a = 97$ nm, $l_{CV} = 20$ nm. Solution contained 1 mM Ru(NH$_3$)$_6$Cl$_3$. The concentration of KNO$_3$, mM: 1000 (green), 500 (yellow), 200 (pink), and 100 (blue; inset).

of FcCH$_2$OH in the cell. Further decrease in ionic strength resulted in a significant potential shift, marked changes in the wave shape, and complete disappearance of the wave at c_{KNO_3} of 1 to 3 mM. A precipitous i_{TLC} drop in response to a small change in electrolyte concentration (e.g., from 100 to 50 mM) points to a strong double layer effect. Since the Debye length is ∼1 nm and ∼1.4 nm for 0.1 and 0.05 M solutions of a 1:1 electrolyte, respectively,[19a] only a minor overlap of two diffuse layers could be expected in the 12-nm-thick TLC. The total charge stored within a diffuse layer (q) can be evaluated (at $T = 25$ °C) as[19a]

$$q = 1.17 \times 10^{-5} Ac^{*1/2} \sinh(19.5\phi_0) \qquad (15)$$

where A is the electrode surface area, c^* is the molar concentration of 1:1 electrolyte, and ϕ_0 is the electrode potential relative to the bulk solution. For $\phi_0 = 100$ mV and $a = 58$ nm, eq 15 yields, for a diffuse layer in the TLC used in Figure 8A and 8B, $q = 1.3 \times 10^{-15}$ C at $c^* = 0.1$ M and 9.5×10^{-16} C at $c^* = 0.05$ M. The charge corresponding to all cationic (or anionic) species contained in the same TLC is Alc^*F, i.e., 1.2×10^{-15} C and 6×10^{-16} C for the same electrolyte concentrations. The above estimate indicates that the number of ions contained in the 12-nm-thick TLC may be sufficient to form two double layers when $c_{KNO_3} = 0.1$ M, but not 0.05 M.

It is plausible that the initial decrease in i_{TLC} that occurred at $c_{KNO_3} = 0.05$ M and was not accompanied by major changes in

Figure 9. Effect of the supporting electrolyte concentration in a larger TLC. $a = 87$ nm, $l_{CV} = 124$ nm. Solutions contained 1 mM Ru(NH$_3$)$_6$Cl$_3$. c_{KNO_3}, mM was as follows: 1000 (1), 500 (2), 200 (3), 100 (4), 50 (5), 10 (6), 5 (7), and 2 (8). The curves obtained at lower electrolyte concentrations were not completely retraceable. For better clarity, only forward portions of some voltammograms are shown.

the half-wave potential and the shape of the voltammogram was caused by the trapping of charged redox species within two double layers and corresponding decrease in diffusion current. At even lower c_{KNO_3} (e.g., 3 mM) the metal/solution interface cannot be properly biased, and therefore no voltammetric wave is observed.

A qualitatively similar behavior was observed in a slightly larger TLC ($a = 97$ nm, $l_{CV} = 20$ nm) containing multicharged cationic Ru(NH$_3$)$_6{}^{3+/2+}$ species (Figure 8C). The increase in i_{TLC} by ∼50% occurred when c_{KNO_3} was lowered from 1000 mM to 200 mM. It is not surprising that the current enhancement by migration for multicharged redox species was observed at higher electrolyte concentrations than that for the FcCH$_2$OH$^{+/0}$ couple despite a somewhat larger l_{CV}. The effect of further c_{KNO_3} decrease is also more dramatic for Ru(NH$_3$)$_6{}^{3+/2+}$: i_{TLC} dropped by a factor of ∼80 when c_{KNO_3} was reduced to 100 mM (inset).

For a TLC with a significantly larger distance between two electrodes, our model predicts that both the increase in i_{TLC} due to the migration effect and its subsequent drop at lower electrolyte concentrations should be smaller. The latter effect should also occur at significantly lower electrolyte concentrations. Both predictions are confirmed by the family of voltammograms of Ru(NH$_3$)$_6{}^{3+/2+}$ obtained in a thicker TLC (Figure 9; $a = 87$ nm, $l_{CV} = 124$ nm). The i_{TLC} value kept increasing while c_{KNO_3} decreased from 1 M to 50 mM, and its subsequent drop at $c_{KNO_3} = 10$ mM was smaller than that in a thinner TLC (cf. Figure 8C).

3.5.3. TLC Voltammograms of Mixed Redox Species. Another unexpected phenomenon was observed in TLC voltammograms of a mixture of two redox mediators. Figure 10A shows steady-state voltammograms obtained at the same 62-nm-radius Pt electrode before etching (blue curve) and after etching (red curve) in solution containing 1 mM Ru(NH$_3$)$_6$Cl$_3$, 1 mM FcCH$_2$OH, and 0.2 M KNO$_3$. As expected, at equal concentrations of Ru(NH$_3$)$_6$Cl$_3$ and FcCH$_2$OH, the heights of their waves are similar (in both curves, the Ru(NH$_3$)$_6{}^{3+}$ wave is a little lower because of a somewhat smaller diffusion coefficient, i.e., 6.7×10^{-6} cm^2/s vs 7.8×10^{-6} cm^2/s[9a]). However, in the TLC voltammogram (Figure 10B), the ruthenium wave is ∼2.7 times higher. This experiment was repeated many times in different nano-TLCs and always yielded a wave height ratio ≥ 2.

The above observation could be explained by preferential accumulation of charged Ru(NH$_3$)$_6{}^{3+}$ species in the nano-cavity, either on the inner glass wall or on a Pt surface, prior to TLC formation. To test the first possibility, several etched
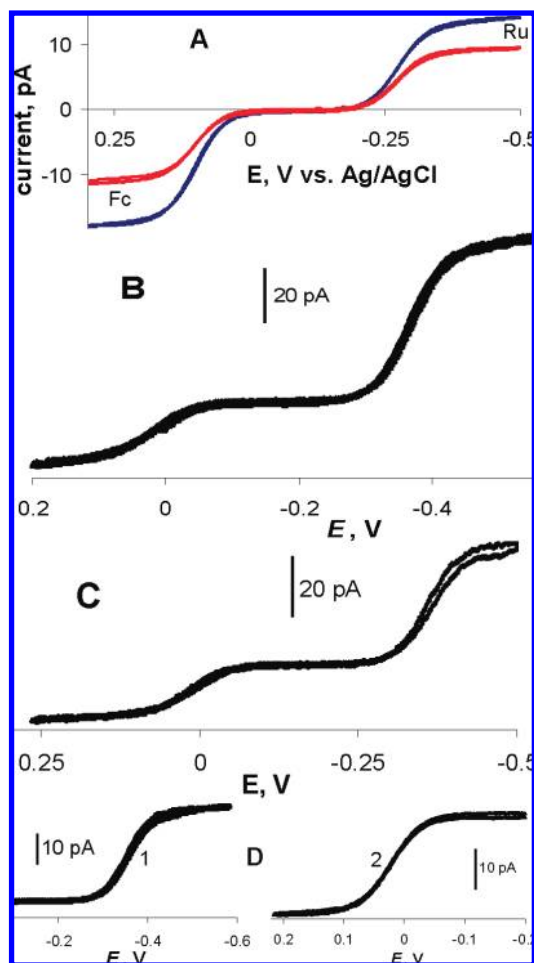
Figure 10. Voltammograms of $Ru(NH_3)_6Cl_3$ and $FcCH_2OH$ obtained at the same 62-nm-radius Pt electrode. (A−C) $c_{Ru(NH_3)_6Cl_3} = c_{FcCH_2OH} = 1$ mM. (A) Voltammograms obtained in the bulk solution before (blue) and after etching (red). (B−D) TLC voltammograms. $l_{CV} = 33$ nm. (D) Solution contained either 1 mM $Ru(NH_3)_6Cl_3$ (1) or 1 mM $FcCH_2OH$ (2). c_{KNO_3} was 0.2 M (A, B) and 1.0 M (C, D).

nanoelectrodes were loaded with solutions of different pH values (from 1 to 7) containing a mixture of $Ru(NH_3)_6Cl_3$ and $FcCH_2OH$. Although the glass wall charge changes markedly over this range of pH (which brackets the isoelectric point),[20] no significant effect of pH on TLC currents was detected. To check the second hypothesis, different potentials (from -0.3 V to $+0.3$ V vs Ag/AgCl) were applied to several etched Pt nanoelectrodes immersed in a solution containing $Ru(NH_3)_6Cl_3$ and $FcCH_2OH$. Each electrode was removed from solution before disconnecting it from the potentiostat and subsequently inserting it into Hg. The electrode potential applied during the solution sampling did not affect the ratio of wave heights in TLC voltammograms.

One of the reasons for the enhanced TLC current of hexaamineruthenium is the effect of migration. Since the migration term in the Nernst−Planck equation is proportional to the square of the ionic charge, this component should be

(20) Wei, C.; Bard, A. J.; Feldberg, S. W. *Anal. Chem.* **1997**, *69*, 4627.
(21) Marcus, R. A. *J. Chem. Phys.* **1965**, *43*, 679.
(22) (a) Hupp, J. T.; Weaver, M. J. *J. Phys. Chem.* **1985**, *89*, 2795. (b) Gennett, T.; Milner, D. F.; Weaver, M. J. *J. Phys. Chem.* **1985**, *89*, 2187.
(23) Rudolph, M.; Reddy, D. P.; Feldberg, S. W. *Anal. Chem.* **1994**, *66*, 589A.

larger for multicharged $Ru(NH_3)_6^{3+/2+}$ species than for $FcCH_2OH^{+/0}$. From Figure 8C, one can see that, at $c_{KNO_3} = 0.2$ M, the $Ru(NH_3)_6^{3+/2+}$ wave was higher than that at 1.0 M but the height of the $FcCH_2OH^{+/0}$ was essentially the same for both electrolyte concentrations (Figure 8A). Thus, the wave height ratio of these redox mediators should decrease with increasing c_{KNO_3}. This behavior can be seen in Figure 10C: at $c_{KNO_3} = 1.0$ M, the ratio of the $Ru(NH_3)_6^{3+/2+}$ and $FcCH_2OH^{+/0}$ wave heights is 2.1 as opposed to 2.7 at $c_{KNO_3} = 0.2$ M (Figure 10B).

The remaining difference between ruthenium and ferrocene wave heights at $c_{KNO_3} = 1$ M cannot be attributed to migration. Interestingly, the heights of voltammetric waves of $Ru(NH_3)_6^{3+/2+}$ and $FcCH_2OH^{+/0}$ obtained independently are similar (Figure 10D). In this case, TLCs were formed by sampling either $Ru(NH_3)_6Cl_3$ (curve 1) or $FcCH_2OH$ (curve 2) rather than a mixture of the two electroactive species. This observation suggests that the increased height of the $Ru(NH_3)_6^{3+/2+}$ wave is caused by interaction of two redox mediators. We hypothesized that a rapid homogeneous reaction between $Ru(NH_3)_6^{2+}$ generated at a Pt surface and $FcCH_2OH^+$ produced at Hg

$$Ru(NH_3)_6^{2+} + FcCH_2OH^+ = Ru(NH_3)_6^{3+} + FcCH_2OH$$
(16)
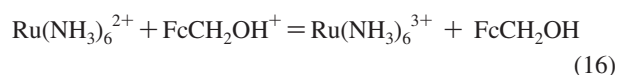
may result in the i_{TLC} increase. However, digital simulations using DigiSim 3.03 (Bioanalytical Systems, West Lafayette, IN)[23] showed that such a reaction (EC′ mechanism) should not affect the TLC current as long as the diffusion coefficients of redox species are similar. A higher level model is needed to fully explain the differences between $Ru(NH_3)_6^{3+/2+}$ and $FcCH_2OH^{+/0}$ TLC voltammograms. One should note that a very small volume and high mass transfer rate make nano-TLCs potentially useful for studying rapid coupled kinetics. In a sufficiently small TLC, it may be possible to detect homogeneous reactions between individual molecules.

4. Conclusions

Electrochemical TLCs were prepared by inserting slightly recessed, etched nanoelectrodes filled with aqueous solution into dry mercury. Voltammetry and SECM were used to evaluate the cell thickness and radius. Quantitative electrochemical experiments in nano-TLCs were carried out using five different redox mediators. An extremely small (zeptoliter) TLC volume allows sampling and detection of individual molecules, as well as studying various physicochemical processes (e.g., adsorption and heterogeneous electron transfer) at the level of single molecules. The responses of nano-TLCs, even very small ones with $a \leq 10$ nm and $l \leq 10$ nm, could be fitted to the classical electrochemical theory.

Several unusual electrochemical phenomena observed in nano-TLCs are related to their size and unique properties. Among them are the current rectification due to nonpolarizability of the Hg electrode; strong dependence of the response on concentration of supporting electrolyte when the number of ionic species inside TLC becomes too small for the formation of two electrical double layers; and an enhanced voltammetric response to one redox species relative to the other. TLCs can be used as nanoreactors to conduct various electrochemical and chemical processes under controlled experimental conditions including spatial constrains, a strong and adjustable electric field, and very fast mass transport.

Supporting Information Available: Derivation of eq 9. This material is available free of charge via the Internet at http://pubs.acs.org.

JA711088J